# Ⅲ-3

## Atoms and Molecules

BL3U

# In-Situ Observation of Electrochemical Reaction by Soft X-Ray Absorption Spectroscopy with Potential Modulation Method

M. Nagasaka, H. Yuzawa, T. Horigome and N. Kosugi
*Institute for Molecular Science, Myodaiji, Okazaki 444-8585, Japan*

For understanding the electrochemical reaction, it is most important to investigate local structures of electrolytes including electric double layers at different potentials. Soft X-ray absorption spectroscopy (XAS) is an element specific method to study local electronic structures of solutions and interfaces. Recently, we developed a liquid cell for XAS in transmission mode [1], in which the thickness of the liquid layer is controllable between 20 and 2000 nm. In addition, we successfully measured XAS of electrolytes in electrochemical reaction by using a liquid cell with built-in electrodes [2]. From the Fe L-edge XAS spectra of aqueous iron sulfate solutions in electrochemical reaction, we revealed change in the valence of Fe ions at different potentials, where each XAS spectrum was measured at a constant potential and the scanning rate of the potential (0.08 mV/s) was quite slower than that in regular cyclic voltammetry (CV) (typically 100 mV/s). In this study, we have developed a potential modulation method to make possible in-situ XAS observation of electrochemical reaction at the same scanning rate of CV.

In the XAS measurement with a potential modulation method, the electrode potential is swept at a fixed photon energy, and soft X-ray absorption coefficients at different potentials are measured at the same time. After repeating the potential modulation at different photon energies, we can get XAS of electrolytes in electrochemical reaction at the same scanning rate of CV.

The experiments were performed at BL3U. XAS spectra of electrolytes were measured by using a liquid cell with built-in electrodes [2]. Figure 1 shows the Fe L-edge XAS spectra of aqueous iron sulfate solutions in electrochemical reaction at 100 mV/s. By increasing the potential from 0.0 to 1.0 V, the peak intensity of Fe(II) (708 eV) is decreased and that of Fe(III) (710 eV) is increased by the oxidation of Fe(II). By decreasing the potential from 1.0 to -0.4 V, the peak intensity of Fe(II) is increased, and that of Fe(III) is instead decreased by the reduction of Fe(III).

To obtain the fraction of Fe(II) and Fe(III) ions, the Fe L-edge XAS spectra at different potentials are fitted by superposition of the reference XAS spectra of Fe(II) and Fe(III) ions. Figure 2 shows fractions of Fe(II) and Fe(III) ions in electrochemical reaction at 100 mV/s. By increasing the potential, the fraction of Fe(III) is increased and that of Fe(II) is decreased. The Fe(II) ions are partially changed to the Fe(III) ions by the oxidation process. It is because a thick liquid layer is necessary for XAS of dilute Fe ions in transmission mode. As shown in the inset of Fig. 2, the XAS spectra includes both the solid-liquid interface that occurs the Fe redox reaction and the bulk electrolyte of Fe(II) that does not involve the electrochemical reaction. The mechanism of these Fe redox process will be discussed by correlating the XAS results with those at the different scanning rates.

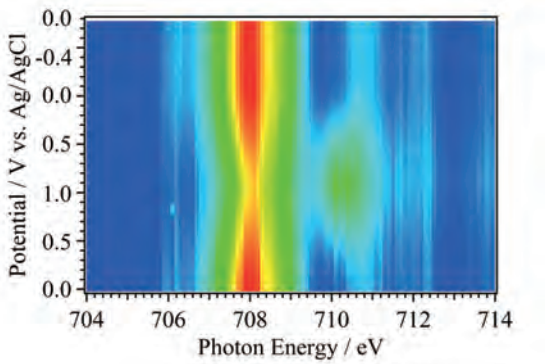


Fig. 1. Two dimensional plots, photon energy and potential (versus Ag/AgCl), of the Fe L-edge XAS spectra in electrochemical reaction of aqueous iron sulfate solutions at the scanning rate of 100 mV/s.

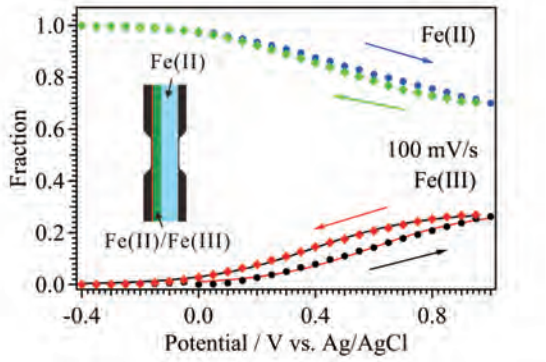


Fig. 2. Fractions of Fe(II) and Fe(III) ions as a function of potential (versus Ag/AgCl) in electrochemical reaction at 100 mV/s. The inset shows a partial oxidation model in a liquid cell.

[1] M. Nagasaka *et al.*, J. Electron Spectrosc. Relat. Phenom. **177** (2010) 130.
[2] M. Nagasaka *et al.*, J. Phys. Chem. C **117** (2013) 16343.

BL3U

# Interaction of Pyridine with Water in Aqueous Solution Studied by Soft X-Ray Absorption Spectroscopy in C and N K-edges

M. Nagasaka, H. Yuzawa and N. Kosugi
*Institute for Molecular Science, Myodaiji, Okazaki 444-8585, Japan*



Pyridine is liquid and is soluble in water at any concentration. In aqueous pyridine solution, the formation of hydrogen bond (HB) between the N site of pyridine and the H site of water is proposed by the vibrational spectroscopy [1]. But the local structure of pyridine-water mixture is unknown. Soft X-ray absorption spectroscopy (XAS) is an element specific method applicable to the local structure study. In the present work, we have measured the C and N K-edge XAS of pyridine-water mixtures at different concentrations, and investigated the interaction of the C and N sites of pyridine with water in the binary solutions.

The experiments were performed at BL3U. XAS of liquid samples were measured by a transmitted-type liquid cell at 25 °C [2]. The liquid layer was sandwiched between two 100 nm-thick $Si_3N_4$ membranes. The thickness of the liquid layer is controllable between 20 and 2000 nm by adjusting the He backpressure.

Figure 1(a) shows the C K-edge XAS of pyridine gas and pyridine-water solution $(C_5H_5N)_X(H_2O)_{1-X}$. The transition C 1s → π* shows two peaks: First peak (C1) is derived from the *meta*- and *para*-C sites of pyridine. The second peak (C2) is the *ortho*-C sites. From gas to liquid pyridine (X=1.0), both the C1 and C2 peaks are shifted to the lower photon energy. Figure 1(b) shows the N K-edge XAS of pyridine gas and pyridine-water solutions. The N 1s → π* peak shows the higher energy shift from gas to liquid. These energy shifts are consistent with those of the pyridine clusters with an antiparallel structure [3], but are smaller than in the cluster case.

By increasing the molar fraction of water in pyridine-water solution, the XAS peaks are shifted as shown in Fig. 1. Table 1 shows the peak shifts of pyridine-water mixtures from that of liquid pyridine. The C1 peaks related to the *meta*- and *para*-C sites are not changed at different concentrations. The C2 peaks related to the *ortho*-C sites are slightly shifted to the higher photon energy by increasing the molar fraction of water. The N peaks are more evidently shifted to the higher photon energy. These energy shifts are reasonable, assuming that the energy shift arises from HB between the N site of pyridine and water in the pyridine-water binary solutions. The order of the magnitude of the peak energy shift (N > C2 > C1) is caused by weakening the influence of HB interaction of water at each site of pyridine with father from the N site of pyridine.

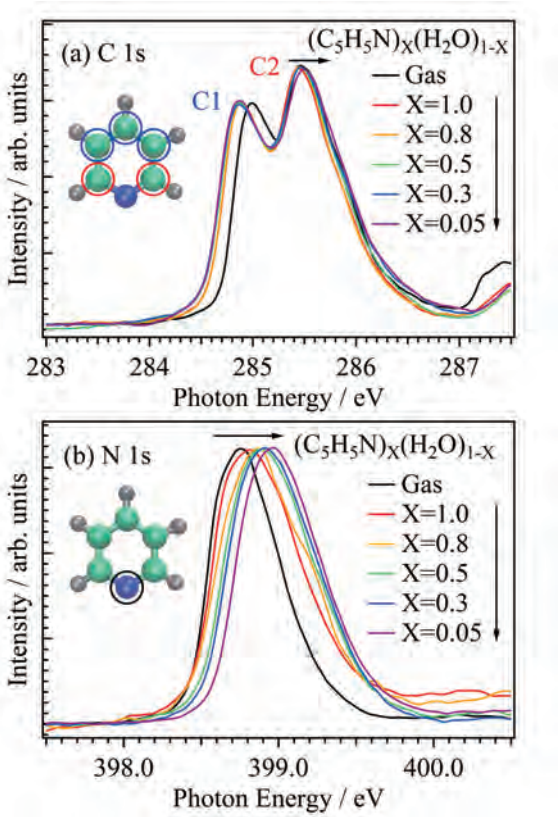


Fig. 1. XAS spectra of pyridine-water mixtures at different concentrations in (a) C and (b) N K-edges. The XAS spectra of pyridine gas are also shown. The peaks are shifted to the direction of arrows by increasing the molar fraction of water.

Table 1. Peak energy shifts (eV) of pyridine-water mixtures from liquid pyridine (X=1.0).

| $(C_5H_5N)_X(H_2O)_{1-X}$ | C1 | C2 | N |
|---|---|---|---|
| Gas | 0.10 | 0.04 | -0.08 |
| X=1.0 | – | – | – |
| X=0.8 | 0.00 | 0.01 | 0.04 |
| X=0.5 | -0.02 | 0.02 | 0.08 |
| X=0.3 | -0.02 | 0.02 | 0.10 |
| X=0.05 | -0.02 | 0.05 | 0.14 |

[1] S. Schlücker *et al.*, J. Phys. Chem. A **105** (2001) 9983.
[2] M. Nagasaka *et al.*, J. Electron Spectrosc. Relat. Phenom. **177** (2010) 130.
[3] I. L. Bradeanu *et al.*, J. Phys. Chem. A **112** (2008) 9192.

BL3U

# Soft X-Ray Absorption Spectroscopic Study of Solid-Liquid Interface

H. Yuzawa, M. Nagasaka and N. Kosugi
*Institute for Molecular Science, Okazaki 444-8585, Japan*

Detailed understanding of the interface interaction is important to clarify physical and chemical phenomena such as molecular adsorptions, catalytic reactions and so on. However, the solid/liquid interface is difficult to measure because it involves two different condensed phases. We generally use particle (electron, ion etc.) or light (IR, X-ray etc.) probe to investigate geometric and electronic structures, but the former interacts too strong with both phases to observe the interface. The latter only gives average information of the interface and bulk, where the information of the interface (minor component) get covered up by that of the bulk [1]. Thus, new approaches are required to measure the solid/liquid interface.

We developed a transmission-type liquid XAS (X-ray Absorption Spectroscopy) cell with $Si_3N_4$ or SiC windows, which is able to control easily the thickness of the liquid thin layer (20-2000 nm), for the soft X-rays [2]. From the other point of view, this liquid cell contains solid/liquid interfaces and can strengthen the information of the interface for light probe by controlling the liquid thickness. Thus, we tried to detect the interaction of solid/liquid interface in the liquid XAS cell, whose surface is modified to objective structures.

The experiments were carried out in BL3U. Two Au (thickness: 20 nm) and Cr (5 nm) deposited $Si_3N_4$ (100 nm) membranes were used as liquid cell windows. The model surface in this study was prepared by the modification (chemisorption) of 1H, 1H, 2H, 2H -perfluorodecanethiol (F-thiol) monolayer on the gold surface (Fig. 1).

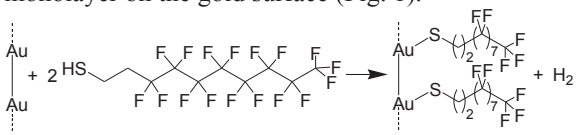


Fig. 1. Modification of gold surface by F-thiol monolayer.

Then, the cell was filled with liquid (water or benzene) and C K-edge XAS was measured at room temperature as shown in Fig. 2.

Figure 3 shows the C K-edge XAS spectra of the modified liquid cell filled with water (blue line) or benzene (red line). In both cases, three absorption peaks (> 290 eV), which correspond to the excitation from C 1s to σ* of F-thiol, were observed. It was confirmed that this system could detect the soft X-ray absorption of molecule at the solid/liquid interface. Nevertheless, the energy positions of each absorption peak were consistent regardless of liquid phase.

On the other hand, when the absorption peak (285.1 eV, 1s→π*) of benzene (green line) extracted from the red line was compared with that without the liquid cell modification of F-thiol (black line), the width of the absorption peak broadened. This would be because the electronic state of benzene molecule was influenced by the interactions between the F atom in F-thiol and the benzene molecule at the interface, e.g., -F···H- interaction [3] and -F···π interaction [4]. Thus, the trace of the interface interaction could be detected in the liquid side.

Through the above experiments, we can conclude that the transmission soft X-ray XAS approach has a potential to detect the interaction of solid/liquid interface.

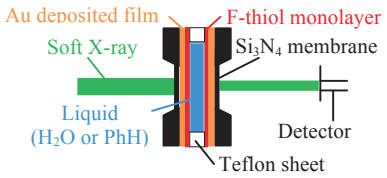


Fig. 2. Schematic (side view) of soft X-ray XAS measurement to detect the interaction at the solid/liquid interface.

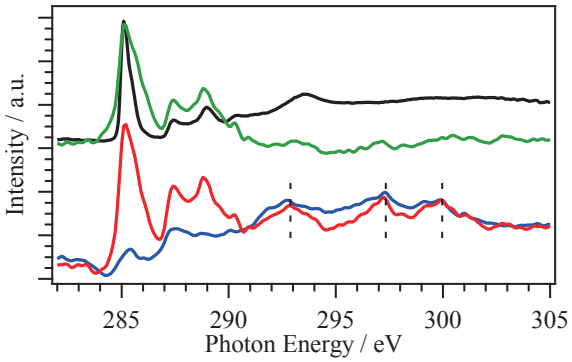


Fig. 3. C K-edge XAS spectra of the modified liquid cell filled with water (blue line) or benzene (red line) and that of the unmodified one filled with benzene (black line). Green line corresponds to the spectrum of the red line subtracted by that of the blue line to remove the influence of the absorption of F-thiol.

[1] F. Zaera, Chem. Rev. **112** (2012) 2920.
[2] M. Nagasaka *et al.*, J. Electron Spectrosc. Relat. Phenom. **177** (2010) 130.
[3] M. D. Prasanna *et al.*, Cryst. Eng. **3** (2000) 135.
[4] B. Brammer *et al.*, New J. Chem. **23** (1999) 965.

BL3U

# Interaction of Acetonitrile with Water in Aqueous Solution Studied by Soft X-Ray Absorption Spectroscopy in C and N K-edges

M. Nagasaka, H. Yuzawa and N. Kosugi
*Institute for Molecular Science, Myodaiji, Okazaki 444-8585, Japan*



Acetonitrile is liquid and is soluble in water at any molar fraction. In aqueous acetonitrile solution, two models of the acetonitrile-water dimer were proposed [1]: One is a hydrogen bond structure between the N site of acetonitrile and the H site of water. The other is a dipole-bonded structure that water is parallel to the C≡N group of acetonitrile by the dipole interaction. Huang *et al.* measured the O K-edge X-ray absorption spectra (XAS) [2] and proposed that the dipole-bonded dimer is abundant compared to the hydrogen bond structure. However, the interaction has not yet been studied from the acetonitrile side. In this study, we have measured the C and N K-edge XAS of acetonitrile-water solutions at different concentrations, and revealed the interaction of the C≡N group of acetonitrile with water.

The experiments were performed at BL3U. XAS of liquid samples were measured by a transmitted-type liquid cell [3]. The liquid layer was sandwiched between two 100 nm-thick $Si_3N_4$ membranes. The thickness of the liquid layer is controllable between 20 and 2000 nm by adjusting the He backpressure.

Figure 1 shows the C and N K-edge XAS spectra of acetonitrile gas and acetonitrile-water solution $(CH_3CN)_X(H_2O)_{1-X}$. From gas to liquid acetonitrile (X=1.0), both the C 1s → C≡N π* and N 1s →C≡N π* peaks are shifted to the higher photon energy. It is because liquid acetonitrile shows the antiparallel structure between the C≡N groups of acetonitrile by the dipole interaction.

Table 1 shows the peak shifts of acetonitrile-water mixtures from that of liquid acetonitrile. The C peak is shifted to the higher photon energy by increasing the molar fraction of water. On the other hand, the N peak is shifted to the lower photon energy. The interaction of the C site of the C≡N group is increased by water, and that of the N site is slightly decreased. These results suggest that the acetonitrile-water solution may have the dipole-bonded structure, in which the oxygen site of water is close to the C site of the C≡N group of acetonitrile. It should be also noted that the peak width at X=0.05 is narrower than those at different molar fractions, suggesting that in dilute aqueous solutions acetonitrile molecules may be isolated by the dipole interaction with water molecules.

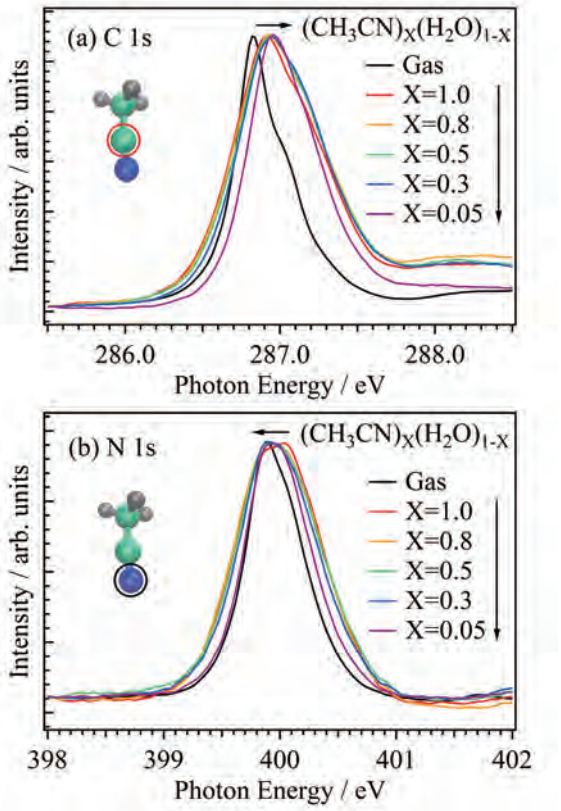


Fig. 1. XAS spectra of acetonitrile-water mixtures at different concentrations in (a) C and (b) N K-edges. The XAS spectra of acetonitrile gas are also shown. The peaks are shifted to the direction of arrows by increasing the molar fraction of water.

Table 1. Peak energy shifts (eV) of acetonitrile-water mixtures from liquid acetonitrile (X=1.0).

| $(CH_3CN)_X(H_2O)_{1-X}$ | C | N |
|---|---|---|
| Gas | -0.09 | -0.09 |
| X=1.0 | – | – |
| X=0.8 | 0.02 | -0.02 |
| X=0.5 | 0.02 | -0.02 |
| X=0.3 | 0.02 | -0.03 |
| X=0.05 | 0.05 | -0.03 |

[1] I. Bakó, T. Megyes and G. Pálinkás, Chem. Phys. **316** (2005) 235.
[2] N. Huang *et al.*, J. Chem. Phys. **135** (2011) 164509.
[3] M. Nagasaka *et al.*, J. Electron Spectrosc. Relat. Phenom. **177** (2010) 130.

BL3B, BL5B, BL7B

# Absorption Measurement of Amino Acid Films Using a Novel *in situ* Vacuum Sublimation System

K. Ishiyama, Y. Tanigawa, S. Takenaka and K. Nakagawa
*Graduate school of Human Development and Environment, Kobe University, Kobe 657-8501, Japan*

It was suggested by Platzman [1] that the magnitude of radiation effect by high energy particle radiation is proportional to

$$\int_0^T \frac{df}{dE}\frac{dE}{E} ,$$

where, $T$ the kinetic energy of particle, $f$ the oscillator strength and $df/dE$ is the oscillator strength distribution which is proportional to the absorption cross section $\sigma$. Since $T$ is sometimes order of MeV, we need to measure $\sigma(E)$ for 5 eV<$E$<1 MeV. Synchrotron radiation is very powerful tool to measure such wide-energy-range absorption spectra.

One of difficulties to measure $\sigma(E)$ within such wide energy range is the large dynamic range of $\sigma$ ($E$). For example, for alanine film, $\sigma$ ($E$=17eV) =1.2x10$^{-16}$ cm$^2$ and $\sigma$ ($E$=250eV) =6.8x10$^{-19}$ cm$^2$ ; the ratio is 5600. Thus in order to obtain the reliable spectrum, we must change the film thickness over 20 times. In order to do this, we developed a novel *in situ* sublimation system (Fig. 1). Substrate is made of Kapton film with very small heat capacity, which is helpful to prevent overheat. Wide area of substrate allows us to get the high sublimation yield.

Figure 2 shows an example of absorption spectrum of glutamine measured at BL-5B. First we measured with the grating 2 and the mirror 4 (G2M4) plus the aluminum filter. After that we changed the measurement system to G2M4 and added the thickness of the same glutamine film to get the spectrum designated by "G2M4". Repeating this procedure, we obtained four spectra shown in Fig. 2. Thickness of "G2M1" film was roughly estimated to be about 4.5 times of "G2M4+Al" film.

Connecting four spectra in Fig. 2, we determined the experimental data as shown in Fig. 3.

Using the *in situ* sublimation system, we will complete the measurement of 20 amino acid molecules, among which several spectra were already reported [2].

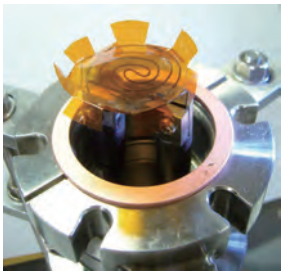

Fig. 1. A novel *in situ* sublimation system.

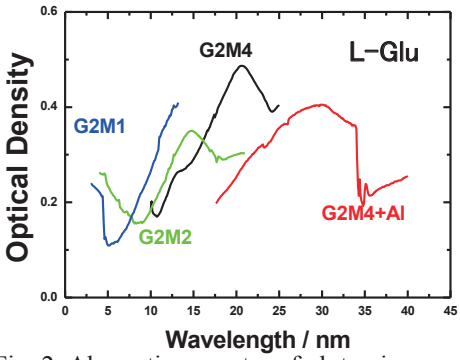


Fig. 2. Absorption spectra of glutamine measured at BL5B.

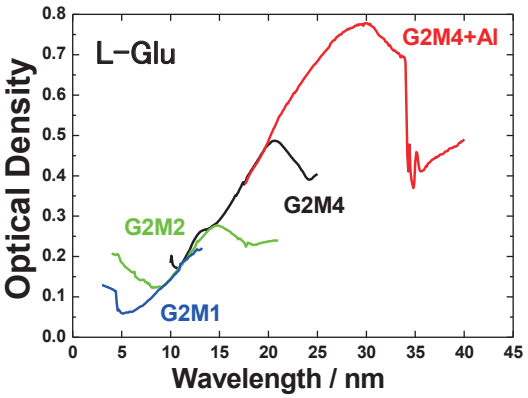


Fig. 3. Determined experimental data.

[1] R. L. Platzman, Vortex, **23** (1962) 372.
[2] M. Kamohara, Y. Izumi, M. Tanaka, K. Okamoto, M. Tanaka, F. Kaneko, Y. Kodama, T.Koketsu and K. Nakagawa, Rad. Phys. Chem. **77** (2008) 1153.

BL4B

# Multi-Electron-Ion Coincidence Spectroscopy by Using a Magnetic Bottle Electron Spectrometer

I. Umekawa[1], Y. Shibata[1], K. Soejima[1], E. Shigemasa[2] and Y. Hikosaka[1]
[1] *Department of Environmental Science, Niigata University, Niigata 950-2181, Japan*
[2] *UVSOR Facility, Institute for Molecular Science, Okazaki 444-8585, Japan*



A doubly-charged molecular ion can be formed by double photoionization in which two electrons are released from the molecule by absorbing a photon with energy above the double ionization potential. Such molecular dication states are inherently dissociative due to the Coulomb repulsion between the two positive charges, though the lifetimes are different from the electron states and further from the vibrational levels. While the information of the lifetimes is important in simulations of atmosphere compositions [1], experimental determinations of the lifetimes depending on vibronic states are still limited even for simple molecules.

In this work, we have developed an electron-ion coincidence spectrometer, with an aim to investigate the stabilities of individual vibronic states in molecular dications. The coincidence spectrometer is based on a magnetic-bottle time-of-flight electron spectrometer [2], which schematic is shown in Fig. 1. Electrons produced by photoionization of sample molecules are collected by an inhomogeneous magnetic field over 4π solid angle, and their kinetic energies are determined from the times of flight to a micro channel plate detector. At 10 μs later than the incidence of the photoionization light pulse, pulsed high voltages are applied to the electrodes placed across the photoionization region, which extracts the ions staying in the ionization region toward the same detector.

Figure 2 shows a time-of-flight spectrum measured for $CO_2$ at a photon energy of 59.7 eV, where times-of-flight of electrons (ions) are observed before (after) 10 μs. In the spectrum, a weak peak for double-charged $CO_2^{2+}$ ions can be seen, in addition to mono-cation peaks. The observation of the $CO_2^{2+}$ ions is attributed to the formation of doubly-charged ion states with lifetimes in the order of μs or longer; otherwise, only the fragment ions should be observed due to dissociation before reaching the detector.

In order to investigate the doubly-charged ion states relevant to the metastable $CO_2^{2+}$ ions, kinetic energies of the electron pairs observed in coincidence with the $CO_2^{2+}$ ions are extracted. Figure 3 shows the energy correlations of the electron pairs. Two photoelectrons emitted on double photoionization shares the available energy which is the energy difference of the photon energy and the binding energy of a formed doubly-charge ion state. Thus, the formation of a doubly-charge ion state appears on the energy correlation map as a diagonal structure with a slope of -1. In practice, corresponding structures are discernible on the map in Fig. 3 around (faster electron energy) + (slower electron energy) = 20 eV. The binding energies of doubly-charge ion states relevant to the metastable $CO_2^{2+}$ are determined to 40 eV, which confirms a previous measurement [3]. We plan further measurements, as detailed discussion needs higher statistics in the coincidence data.

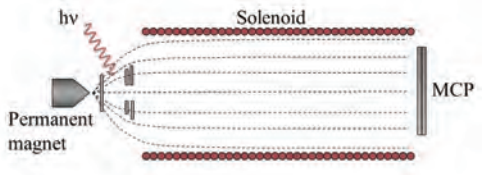


Fig. 1. Schematic of the electron-ion coincidence spectrometer.

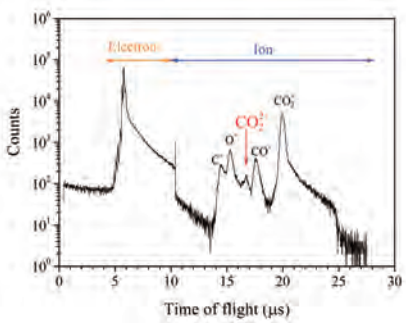


Fig. 2. Time-of-flight spectrum measured for $CO_2$ at a photon energy of 59.7 eV, where times-of-flight of electrons (ions) are observed before (after) 10 μs.

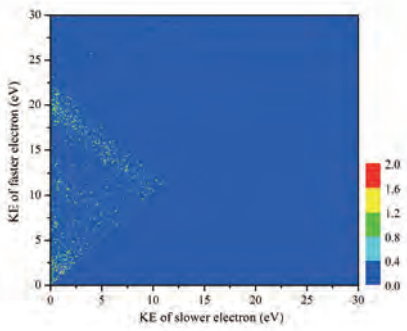


Fig. 3. Energy correlation between two photoelectron observed in coincidence with metastable $CO_2^{2+}$ ions.

[1] R. Thissen *et al.*, Phys. Chem. Chem. Phys. **13** (2011) 18264.
[2] A. Matsuda *et al.*, Rev. Sci. Instrum. **82** (2011) 103105.
[3] A. E. Slattery *et al.*, J. Chem. Phys. **122** (2005) 084317.

BL6U

# The Observation of Doppler Profile of Photoelectrons Emitted from Rydberg Oxygen Atom Following O 1s Inner-Shell Excitation of $CO_2$

T. Gejo[1], K. Myojin[1], T. Tajiri[1], K. Maekawa[1], K. Honma[1], H. Iwayama[2] and E. Shigemasa[2]
[1]*University of Hyogo, Ako-gun 678-1297, Japan*
[2]*UVSOR Facility, Institute for Molecular Science, Okazaki 444-8585, Japan*

Molecules following photo-excitation in the vicinity of inner-shell ionization thresholds provides interesting properties. For photon energies just above ionization threshold, an electron can escape from the ion as a slow photoelectron. The core-hole ion, however, immediately undergoes Auger decay, emitting a fast Auger electron. This leads to a drastic increase of the strength of the Coulomb interaction between the slow out-going photoelectron and the residual ion. When the slow electron lose sufficient kinetic energy by this retardation, it become recaptured by the molecular ion into a Rydberg state. The recapture of the photoelectron results in high-n Rydberg states in singly charged ion. After that, the ion undergoes fragmentation. Since the electron in Rydberg states are relatively stable, Rydberg atom can be generated after this ion fragmentation. This can be confirmed by photoelectron spectra in low kinetic energy region, since Rydberg atom may emit the electron by changing its ion core state.

We have investigated low energy photoelectron spectra of $CO_2$ in O 1s excited state region. Since two oxygen atom locate at ends of $CO_2$, one can expect high kinetic energy of Rydberg oxygen atom (O*). As a result, the photoelectron spectra due to O* is expected to show splitting by strong Doppler effect, which gives the information about dynamics of O* generation.

The experiment was performed on the soft X-ray undulator beamline BL6U at UVSOR. To record the electron kinetic energy spectra, we used a hemispherical electron energy analyzer (MBS1) equipped with a gas cell. The resolution of the electron analyzer was set to approximately 8 meV. The typical pressure in the main chamber housing the gas cell was about $1.0 \times 10^{-3}$ Pa during the measurements. The polarization of the incident photon beam generated by the undulator is horizontal and the photoelectron analyzer can be rotated at horizontal or vertical position respect to this polarization. Energy calibration of the incident photon beam was carried out by recording the total ion yield spectrum of $CO_2$ in the vicinity of the O 1s ionization threshold.

Figure 1 shows the photoelectron spectra of $CO_2$ obtained at photoexcitation energies of 538.85, 539.50, 539.90, and 540.65 eV. The peaks clearly show the Doppler splittings, implying that O*s are generated to polarization direction. We have fitted the Doppler profiles with assuming on Gaussian kinetic energy distribution and one β parameter. The result of the fittings provides β ~ 1.2. These results show high preference for parallel direction, which is more than those expected from the β value obtained by the angular distribution of fragment ions, which is 0 ~ 1 at excitation energies around 1s ionization threshold [1]. Thus, these relatively high β values suggest that the absorption due to Σ ← Σ transition is more important role on the generation of O* fragments than Π ← Σ transition. This can be rationalized by that npσ type Rydberg transition is much suitable to generate these O*.

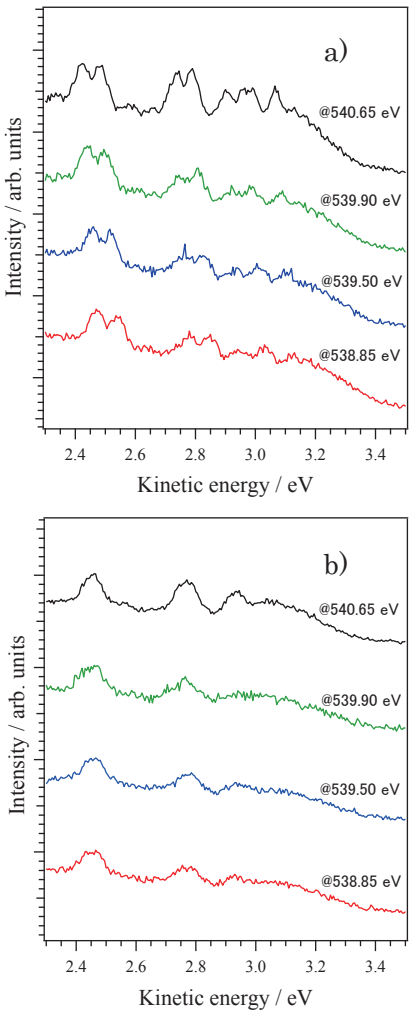


Fig. 1. Photoelectron spectra of Rydberg oxygen atom, following O 1s inner-shell excitation of $CO_2$ The electron analyzer set at a) horizontal and b) vertical position to polarization of SR, and the excitation energies are 538.85, 539.50, 539.90, and 540.65 eV .

[1] K. Okada *et al.,* Phys. Rev. A, **66** (2002) 032503.

BL6U

# Formation of $H_3^+$ Fragment Following Auger Decay in Ethane

Y. Shibata[1], T. Shirota[2], K. Hoshina[2], H. Iwayama[3], E. Shigemasa[3] and Y. Hikosaka[1]
[1]*Department of Environmental Science, Niigata University, Niigata 950-2181 Japan*
[2] *Faculty of Pharmaceutical Sciences, Niigata University of Pharmacy and Applied Life Sciences, Niigata 956-8603 Japan*
[3]*UVSOR Facility, Institute for Molecular Science, Okazaki 444-8585 Japan*

Formation of $H_3^+$ fragment ion has been widely observed in the dissociations of organic molecular dications. The mechanism of the $H_3^+$ formation has absorbed special attention, in connection with rearrangements of the molecular structures due to rapid hydrogen migration [1, 2]. In this work, we have investigated the dication states relevant to the $H_3^+$ formation from $C_2H_6$ molecules, by using an Auger electron-ion coincidence method.

The experiment was performed at the undulator beamline BL6U, by using an Auger electron-ion coincidence spectrometer consisting of a double toroidal electron analyzer and a three-dimensional ion momentum spectrometer [3-5]. Auger electrons ejected at ~54.7º with respect to the electric vector of the incident light were sampled and analyzed in energy by the electron analyzer. According to the detection of each Auger electron, a pulsed electric field was applied to the interaction region, in order to extract the formed ions into an ion momentum spectrometer.

The top panel of Fig. 1 shows a time-of-flight spectrum of ions measured in coincidence with C1s Auger electrons emitted after inner-shell photoionization of $C_2H_6$ molecules. In this spectrum, fragment ion manifolds for the $CH_n^+$ and $C_2H_n^+$ sequences are observed around 1300 ns and 2000 ns, respectively. Below 500 ns, besides the $H_2^+$ peak, a weak peak assignable to $H_3^+$ is discernible. The bottom panel of Fig. 1 shows a two-dimensional map for the correlations between fragment ions detected in coincidence with an Auger electron. Here, an area covering coincidences between $H_3^+$ (vertical axis) and the counterpart ions (horizontal axis) is presented. On the two-dimensional map, clear structures for coincidences between the fragment ion pairs of $H_3^+$+ $C_2H_3^+$ and $H_3^+$+ $C_2H_4^+$ can be identified, while any structure for the pairs of $H_3^+$+ $CH_n^+$, accompanying the C-C bond dissociation, is indiscernible.

Figure 2 shows a C 1s Auger spectrum filtered with the detection of the $H_3^+$+$C_2H_3^+$ ion pair, compared with the total Auger spectrum. The total Auger spectrum exhibits only a broad band structure resulting from overlap of different dication states. One finds that the formation of the $H_3^+$+$C_2H_3^+$ ion pair is associated with low-lying dication states in the binding energy range of 40-55 eV, and the dissociation of the states lying in this range result in the formation of $H_3^+$ fragment. The dication states with the electronic configuration of $1e_g^{-2}$ are known to lie in this binding energy range [6].

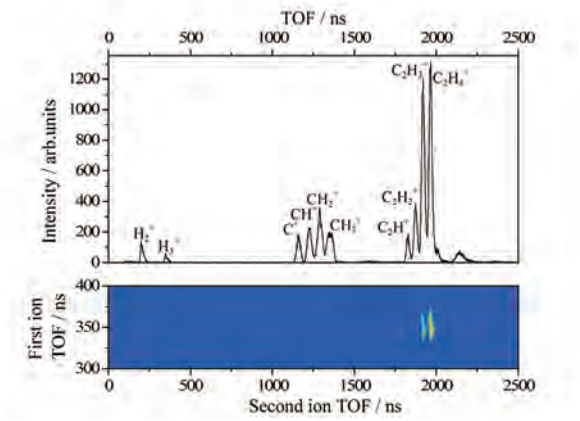


Fig. 1. (Top) Time-of-flight spectrum of ions and (Bottom) two-dimensional map for the correlations between fragment ions, both of which are measured in coincidence with C1s Auger electrons emitted after inner-shell photoionization of $C_2H_6$ molecules.

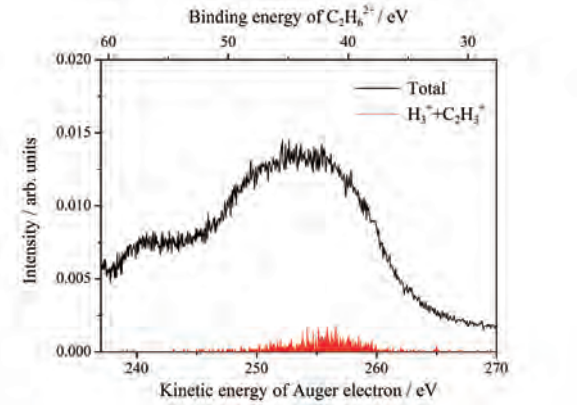


Fig. 2. C1s Auger spectrum of $C_2H_6$ (black), and coincidence Auger spectrum filtered with the formation of the $H_3^+$+$C_2H_3^+$ ion pair (red).

[1] K. Hoshina *et al*., J. Chem. Phys. **134** (2011) 064324.
[2] K. Hoshina *et al*., J. Chem. Phys. **129** (2008) 104302.
[3] T. Kaneyasu *et al*., AIP Conf. Proc. **879** (2007) 1793.
[4] T. Kaneyasu *et al*., J. Electron Spectrosc. Relat. Phenom. **156-158** (2007) 279.
[5] Y. Hikosaka *et al*., submitted.
[6] R. R. Rye *et al*., J. Chem. Phys. **73** (1980) 4867.

BL6U

# Study on Deexcitation Processes Following the Cl 2p Photoexcitation of $CCl_4$ and HCl Molecules Using Two-Dimensional Electron Spectroscopy

H. Iwayama[1], M. N. Piancastelli[2,3,4], D. W. Lindle[5] and E. Shigemasa[1]
[1]*UVSOR Facility, Institute for Molecular Science, Okazaki 444-8585, Japan*
[2]*CNRS, UMR 7614, LCPMR, F-75005, Paris, France*
[3]*Sorbonne Universités, UPMC Univ Paris 06, UMR 7614, LCPMR, F-75005, Paris, France*
[4]*Department of Physics and Astronomy, Uppsala University, PO Box 516, SE- 75120 Uppsala, Sweden*
[5]*Department of Chemistry, University of Nevada, Las Vegas, Nevada 89154-4003, USA*

A molecular inner-shell excitation to the lowest unoccupied anti-bonding orbital is generally followed by two competing processes: molecular dissociation and resonant Auger decay. In particular, for hydrogen halide molecules such as HBr [1] and HCl [2], it has been shown that the molecular dissociation can be faster than the Auger decay. This process is referred to as ultrafast dissociation [1,2]. In their resonant Auger spectra, sharp peaks at electron energies corresponding to the atomic Auger decays have been observed. Two-dimensional electron spectroscopy (2D-ES), in which electron energy spectra are recorded as a function of the photon energy, is one of the most powerful methods to explore the decay dynamics of inner-shell excited molecules. Here we report on the result for the 2D-ES following the Cl *2p* → $7a_1^*$ excitation for $CCl_4$ molecules. As a comparison, we have also measured a 2D map following the Cl *2p* → $\sigma^*$ excitation for HCl molecules.

The experiment was performed on the soft X-ray beamline BL6U at UVSOR. The photon energy resolution E/ΔE was set to 2000. Kinetic energies of the emitted electrons were measured by a hemispherical electron energy analyzer (MBS-A1). The direction of the electric vector was set to be parallel to the axis of the electrostatic lens of the analyzer. The kinetic energy resolution of the analyzer was set to 120 meV. The 2D maps were obtained by taking spectra at a regular photon energy interval of 100 meV across the resonances.

Figure 1 shows the 2D maps for $CCl_4$ and HCl molecules measured in the Cl *2p* excitation region. We can find two sets of five prominent constant kinetic energy lines in the photon energy range from 200 to 204 eV in Fig. 1(b). The two sets correspond to the atomic Auger decays of the Cl $2p_{3/2}^{-1}$ and $2p_{1/2}^{-1}$ states [2]. For the Cl *2p* → $\sigma^*$ excitation of HCl molecules, a large part of Auger decays occurs in the atomic chlorine after the complete dissociation.

Then we look at the 2D map following the Cl *2p* → $7a_1^*$ excitation for $CCl_4$ molecules. As in the case of HCl molecules, we can find two sets of prominent constant kinetic energy lines in Fig. 1(a). Their kinetic energies are the same as those of atomic Auger lines in Fig. 1(b). This means that the ultrafast dissociation process following the Cl *2p* → $7a_1^*$ excitation for $CCl_4$ molecules exists, where the C-Cl bond is broken before the Auger decay. This behavior can be explained by the fact that the $7a_1^*$ orbital of $CCl_4$ has a strong anti-bonding character which plays a similar role as in the case the σ* orbital in HCl. However, we can clearly see other constant kinetic energy lines in Fig. 1(a), which are not observed in Fig. 1(b). They are attributable to the Auger decays from molecular fragments. This fact strongly suggests that the atomic Auger decay is not predominant decay processes for $CCl_4$ molecules. The branching ratio of molecular versus atomic Auger decays depends on the mass of fragments. It is reasonable to consider that the dissociation time for the $CCl_3$ + $Cl^*(2p^{-1}3p^6nl)$ fragmentation following the Cl *2p* → $7a_1^*$ excitation in $CCl_4$ is much longer than that for the H + $Cl^*(2p^{-1}3p^6nl)$ following the Cl *2p* → $\sigma^*$ excitation in HCl. This reasonably explains the present observation.

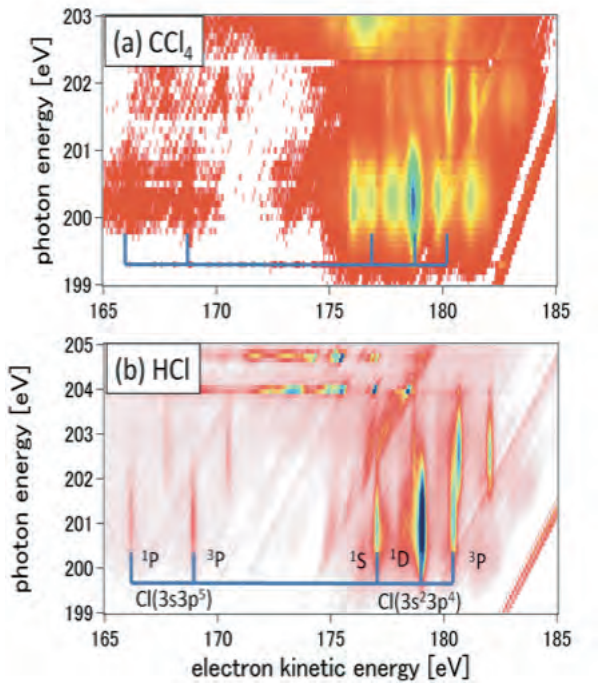


Fig. 1. 2D-PES for (a) $CCl_4$ and (b) HCl molecules measured in the Cl *2p* excitation region.

[1] P. Morin and I. Nenner Phys. Rev. Lett. **56** (1986) 1913.
[2] H. Aksela *et al*., Phys. Rev. A **41** (1990) 600.

BL6U

# Decay Processes Following S 2p Photoexcitation of OCS Studied by High-Resolution Two-Dimensional Electron Spectroscopy

H. Iwayama[1], M. Simon[2] and E. Shigemasa[1]
[1]*UVSOR Facility, Institute for Molecular Science, Okazaki 444-8585, Japan*
[2] *LCPMR, Université Pierre et Marie Curie, 75231 Paris Cedex 05, France*

Molecular inner-shell photoabsorption spectra often exhibit rich structures below the ionization thresholds, which correspond to the excitations of an inner-shell electron into unoccupied valence or Rydberg orbitals. In the case of the molecules composed of light elements, the inner-shell excited states are mainly relaxed via Auger electron emission, and subsequently fragmentation follows in general. Thanks to the continuous works on high-resolution resonant Auger electron spectroscopy, it has been revealed that the nuclear motion of the molecular core-excited states is promoted in competition with the Auger decay.

In the previous report [1], angle-resolved two dimensional (2D) electron spectroscopy, where the resonant Auger-electron spectra are measured as a function of the photon energy, has been applied to the deexcitation processes in the S 2p excitation region of OCS with moderate energy resolution, and compared to the previous work [2]. Here we present the 2D maps following the S $2p_{3/2} \rightarrow \pi^*$ excitation with previously unprecedented resolution.

The 2D measurements were performed at BL6U. The undulator radiation was monochromatized by a variable included angle varied line-spacing plane grazing monochromator. Concerning the 2D electron spectroscopy, the monochromator bandwidth was set to $\Delta E_{Ph}$ ~20 meV at hν=165 eV. Kinetic energy of the emitted electrons was measured by a hemispherical electron energy analyzer (MBS-A1) placed at a right angle with respect to the incident photon beam direction. The direction of the electric vector was set to be either parallel (horizontal) or perpendicular (vertical) to the axis of the electrostatic lens of the analyzer. The energy resolution of the analyzer was set to $\Delta E_k$ ~15 meV.

Figure 1 shows the 2D maps of resonant Auger electron spectra following the S $2p_{3/2} \rightarrow \pi^*$ resonant excitation of OCS measured in horizontal (a) and vertical (b) directions. The diagonal lines in Fig. 1 are attributed to the valence photoelectron lines, which clearly show vibrational side bands indicating that the net energy resolution is far below 50 meV. The peak intensities for the valence photoelectrons in Fig. 1(a) are much stronger than those in Fig. 1(b), indicating that the β values for the valence shells are close to 2 in the vicinity of the S 2p ionization thresholds.

Clear island-like structures elongated in the vertical direction are detected both in Fig. 1(a) and Fig. 1(b) in the kinetic energy region from 144 to 148 eV. Three island-like structures with almost no dispersion between 146.5 and 148 eV have been assigned to three shake-up satellite states [2]. These states are detected mainly in the lower photon energy region and show almost isotropic angular distributions. For the island-like structures with no dispersion in the kinetic energy range from 144 to 146 eV, large differences between Fig. 1(a) and Fig. 1(b) are seen. To our knowledge, no assignments are given to these structures. In order to understand the origins of the structures, sophisticated theoretical calculations are highly desired.

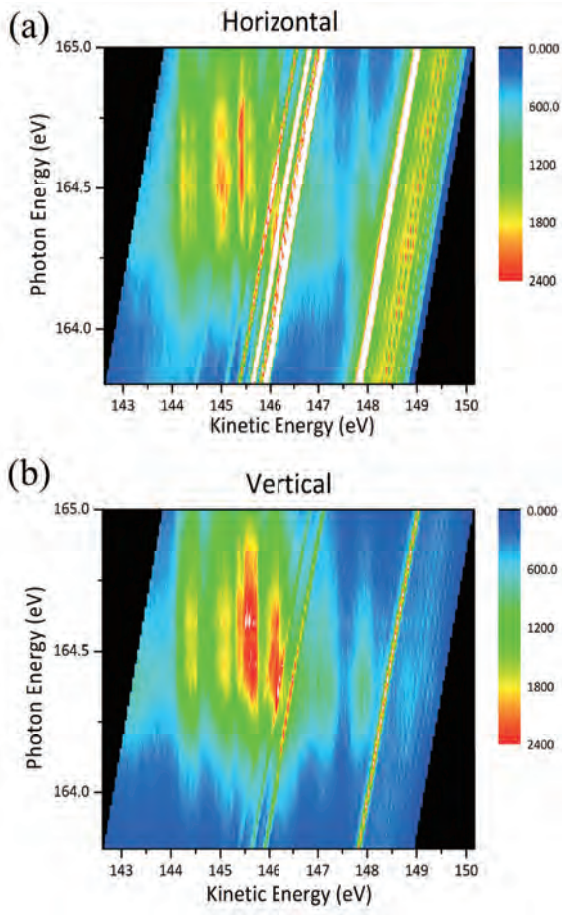


Fig. 1. 2D maps of resonant Auger electron spectra after the S $2p_{3/2} \rightarrow \pi^*$ excitation of OCS, measured at horizontal (a) and vertical (b) directions.

[1] L. Ishikawa, H. Iwayama and E. Shigemasa, UVSOR Activity Report **40** (2013) 61.
[2] S. Masuda, T. Hatsui and N. Kosugi, J. Electron Spectrosc. Rlat. Phenom. **137-140** (2004) 351.

BL6U

# Fluorine K Resonant Auger Decays of *cis*-Hexafluorocyclobutane

T. Kaneda[1], S. Ishikawa[1], K. Okada[1], H. Iwayama[2,3] and E. Shigemasa[2,3]
[1]*Department of Chemistry, Hiroshima University, Higashi-Hiroshima 739-8526, Japan*
[2]*UVSOR Facility, Institute for Molecular Science, Okazaki 444-8585, Japan*
[3]*School of Physical Sciences, Graduate University for Advanced Studies (SOKENDAI), Okazaki 444-8585, Japan*

Inner-shell excited states of molecules relax into various molecular cationic states through Auger decays. The resultant cations are in general unstable and dissociate into fragment ions. Information on the correlation between the Auger-final states and the products provides us deeper insight into the fragmentation dynamics of the inner-shell excited molecules. We found in our previous study that the $C1s^{-1}\sigma_{CC}$* excited *cis*-1,1,2,2,3,4-hexafluorocyclobutane (*cis*-c-$C_4H_2F_6$) molecule decays mainly into the $\sigma_{CC}^{-1}v^{-1}\sigma_{CC}$* states, where $v$ means a $\sigma_{CC}$ or $n_F$ outer-valence orbital, from which fragment ions such as $CHF_2^+$ and $CF^+$ are specifically formed [1]. This report is based on our successive experiments measured in the F 1s excitation region.

The experiments have been performed on the soft X-ray beamline BL6U. The experimental setup has been described in a previous paper [2]. The main chamber was equipped with a pair of a double toroidal electron analyzer (DTA) and an ion time-of-flight mass spectrometer. Synchrotron radiation was irradiated at right angles to the effusive beam of the gaseous *cis*-c-$C_4H_2F_6$ sample. The electrons traveling through the DTA tube were detected with a position sensitive detector (RoentDek, DLD40). The pass energy was set to 400 eV in this study. The electron spectra were acquired at the photon energies including typical resonant peaks as well as at the above-threshold energy of 707.5 eV. The photoelectron spectrum was measured at 684.0 eV for subtracting the contribution from valence ionization. The light intensity at each run was monitored downstream on the beamline. In addition, Auger-electron–photoion coincidence data were obtained at some photon energies.

Figure 1 shows a series of resonant Auger spectra plotted on the final-state energy scale, after subtracting the photoelectron components. The normal Auger spectrum measured under the same experimental conditions is also displayed at the top of Fig. 1 on the double ionization energy (DIP) scale. The DIP value for *cis*-c-$C_4H_2F_6$ is evaluated to be 694.4 eV. The spectra present a great contrast to those in the C 1s region [1]. The resonant Auger spectra resemble the normal Auger spectrum well, indicating that the spectator Auger transitions predominate in the F 1s region. We can assign the intense peak at around 50 eV to the transition to the $n_F^{-1}n_F^{-1}$ final states and at around 70 eV to that to the $F2s^{-1}n_F^{-1}$ states. We also found the peak shifts that change almost linearly with the photon energy. The spectator electron contributes to the screening in the 2-hole-1-electron final states, resulting in the peak shifts towards the higher kinetic energies.

The Auger-electron–photoion coincidence data exhibit that the molecular ion in the $F2s^{-1}n_F^{-1}\sigma^{*1}$ Auger-final states dissociates exclusively into the fragment ions without C–F bonds, namely, $C^+/CH^+$, $C_2H_2^+$ and $F^+$. Further analysis is needed to state conclusive results and is eagerly in progress now.

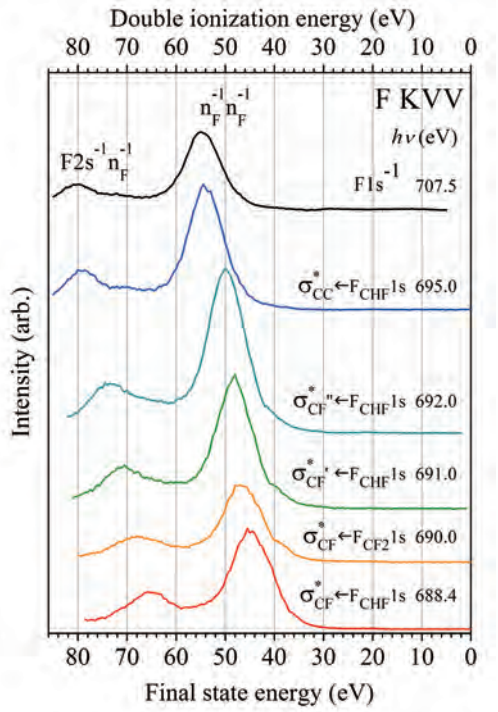


Fig. 1. Resonant Auger spectra of *cis*-c-$C_4H_2F_6$ acquired at a series of photon energies in the F 1s region. The normal Auger spectrum measured at 707.5 eV is also plotted at the top.

[1] S. Ishikawa, K. Okada, H. Iwayama, L. Ishikawa and E. Shigemasa, UVSOR Activity Report 2012 **40** (2013) 58.
[2] T. Kaneyasu, Y. Hikosaka and E. Shigemasa, J. Electron Spectrosc. Relat. Phenom. **156-158** (2007) 279.

BL6U

# Stability of Auger Final Dicationic States Following Core-Ionization of $N_2$ Molecules Studied by an Auger-Electron–Ion Coincidence Method

H. Iwayama and E. Shigemasa
*UVSOR Facility, Institute for Molecular Science, Okazaki 444-8585, Japan*



Absorption of a soft x-ray photon creates a core hole in a molecule. The core hole state is quite unstable and usually decays via Auger-electron emission for light elements. The Auger decay process leads to various dicationic states with two valence holes. Although Auger final dicationic states are generally unstable, and often come apart into ionic fragments due to the Coulomb repulsion between the nuclear charges, metastable dications with lifetimes in microsecond range are known to exist, depending on the nature of their electronic states as shown in Fig. 1. Here we report on the stability of Auger final states following the 1s photoionization of $N_2$ molecules by using an Auger-electron–ion coincidence method.

The Auger-electron–ion coincidence measurements were carried out on the undulator beamline BL6U at UVSOR. The radiation from an undulator was monochromatized by a variable included angle varied line-spacing plane grazing monochromator. The electrons ejected at 54.7° with respect to the electric vector of the incident radiation were analyzed in energy by a double toroidal analyzer (DTA), while ions were extracted from the interaction region into a momentum spectrometer by a pulsed electric field according to the electron detection. Arrival positions on the detector and time-of-flights of ions were recorded for every event. The pass energy of the DTA was set to 200 eV for observing the Auger electrons. The energy resolution was about 1.9 eV. All signals from the detectors were recorded with an 8ch TDC board. The photon energy was set to 450eV.

Figure 2 (a) shows a coincidence map for $N_2^{++}$ and $N^+$ production, in the binding energy region of the dicationic states with two holes in the outer valence orbitals. The vertical and horizontal axes correspond to the kinetic energy of ions and the binding energy of Auger electrons, respectively. Figures 2(b) and 2(c) show the total ion kinetic energy distribution and Auger electron spectrum, which are gained by projecting the counts on the map into the vertical and horizontal axes, respectively. Although the time-of-flights of the $N_2^{++}$ and $N^+$ ions are the same due to the same mass-to-charge ratio, they can easily be distinguished from their kinetic energy differences, as seen in Figs. 2(a) and (b). The peak at 0 eV in Fig. 2(b) is relevant to the metastable $N_2^{++}$ ions, while that centered at 6 eV is associated with the $N^+$ ions.

For ($N^+$, $N^+$) fragmentation processes, a strong correlation between Auger-electron binding energies and ion kinetic energies is detected in Fig. 2(a). The slope of -1, which is represented by the broken line, means that these fragmentation processes correlate to the same dissociation limit. According to the NIST Atomic Database, the corresponding dissociation limit is $N^+(^3P) + N^+(^3P)$.

It is seen in Fig. 2(a) that the Auger final states ranging from 50 to 54 eV lead to $N^+(^3P) + N^+(^3P)$. According to the theoretical work [1], these Auger final states are mainly attributed to the $1\pi_u^{-2}$ configuration. Since the $1\pi_u$ orbital has strong bonding character, it is reasonable that the $1\pi_u^{-2}$ dicationic states lead to the dissociation. It also turns out that the Auger final states ranging from 46 to 50 eV and from 54 to 56 eV result in the production of $N_2^{++}$. These Auger final states are mainly attributable to the $3\sigma_g^{-2}$ and $3\sigma_g^{-1}1\pi_u^{-1}$ configurations.

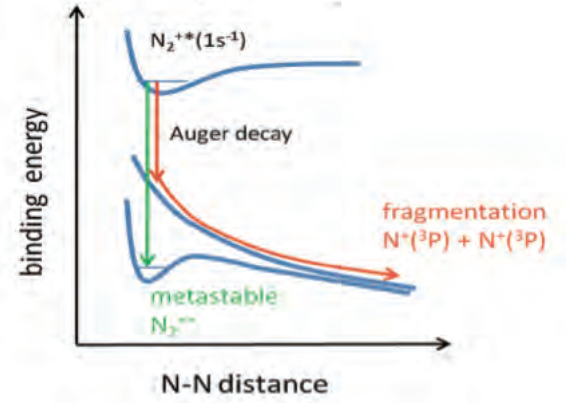


Fig. 1. A schematic representation of core ionization and subsequent decay processes in $N_2$.

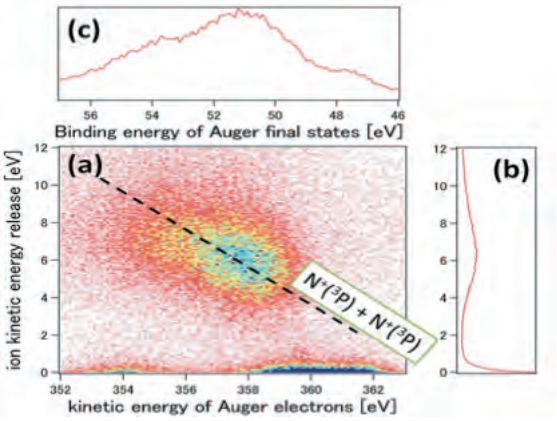


Fig. 2. (a) Auger-electron–ion coincidence map for $N_2^{++}$ and $N^+$ production. (b) and (c) represent the total ion kinetic distribution and Auger electron spectrum plotted on a binding energy scale, respectively.

[1] H. Agren, J. Chem. Phys. **75** (1982) 1267.

BL6U

# Decay Dynamics of Core-Excited HCl and $H_2S$

M. N. Piancastelli[1,2,3], D. W. Lindle[4], R. Guillemin[1,2], M. Simon[1,2], H. Iwayama[5] and E. Shigemasa[5]

[1]*CNRS, UMR 7614, Laboratoire de Chimie Physique-Matière et Rayonnement, F-75005, Paris, France*
[2]*Sorbonne Universités, UPMC Univ Paris 06, UMR 7614, Laboratoire de Chimie Physique-Matière et Rayonnement, F-75005, Paris, France*
[3]*Department of Physics and Astronomy, Uppsala University, PO Box 516, SE- 75120 Uppsala, Sweden*
[4]*Department of Chemistry, University of Nevada, Las Vegas, Nevada 89154-4003, USA*
[5]*UVSOR Facility, Institute for Molecular Science, Okazaki 444-8585, Japan*

We have obtained high-resolution resonant Auger spectra in two isolated systems, HCl and $H_2S$, following Cl 2p and S 2p core excitation respectively. The experimental results have been obtained as 2D maps, namely by taking decay spectra at many photon energy values spaced by 100 meV across the below-threshold resonance regions up to above threshold. The 2D maps allow one to follow in detail the evolution of the spectral features, in terms of relative intensity and dispersion law. We have already successfully applied the same method to another molecular system, namely $CF_4$ [1].

In Figs. 1 and 2 we show the 2D maps for HCl and $H_2S$. A wealth of spectral structures is present below threshold in both cases. The different dispersion law (linear versus nonlinear behavior) is indicative of spectral features related to molecular parent ions or to fragments, $Cl^+$ in HCl and $HS^+$ in $H_2S$. The interpretation of the spectral features is under way.

Together with the spectral assignment, another goal of the present experiments is to compare the data obtained at UVSOR with another data set at the moment under acquisition at the beam line GALAXIES [2], SOLEIL, France.

There we will obtain 2D maps for the same systems, but after 1s core excitation followed by radiative Kα decay. The intermediate state will be the same ($2p^{-1}$LUMO or $2p^{-1}$Rydberg), but prepared via two different pathways, so we will be able to detect subtle differences in the final states due to the different decay dynamics in the two cases. In particular, we have already demonstrated for HCl that during the lifetime of the Cl 1s→LUMO core-excited state some nuclear motion takes place, resulting in a stretch of the H-Cl chemical bond of about 0.1 A [3]. Therefore the internuclear distance in the Cl $2p^{-1}$LUMO core-excited state should be different if such state is reached by direct photoexcitation or by Cl 1s→LUMO excitation followed by Kα decay. We expect to locate the signature of such difference in the decay spectra.

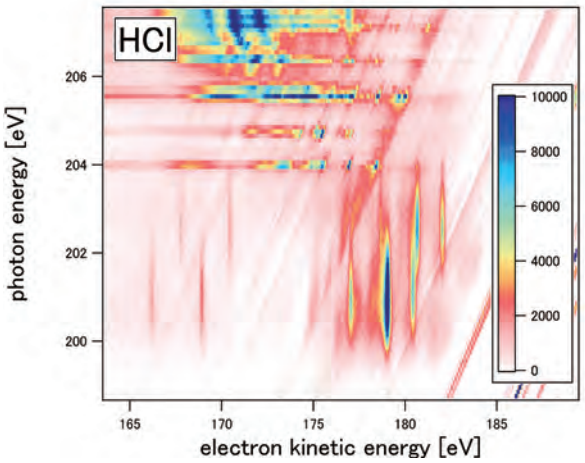


Fig. 1. 2D map for HCl around the Cl 2p threshold.

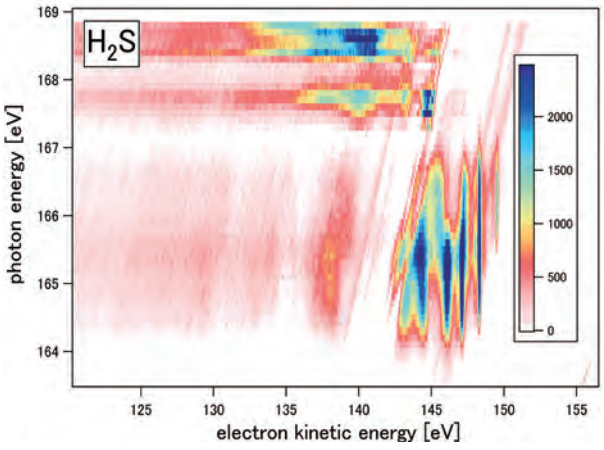


Fig. 2. 2D map for $H_2S$ around the S 2p threshold.

[1] M. N. Piancastelli, R. Guillemin, M. Simon, H. Iwayama, and E. Shigemasa, J. Chem. Phys. **138** (2013) 23430.
[2] D. Céolin *et al.*, J. Electron Spectrosc. Relat. Phenom. **90** (2013) 188.
[3] M. Simon *et al.*, Phys. Rev. A **73** (2006) 020706.

BL6U

# 3d Hole Decay of the Isoelectronic Br and $Kr^+$ $3d^{-1}4s^24p^6$ Configurations

P. Lablanquie[1], H. Iwayama[2], K. Soejima[3] and E. Shigemasa[2]
[1]*LCPMR, Université Pierre et Marie Curie, 75231 Paris Cedex 05, France*
[2]*UVSOR Facility, Institute for Molecular Science, Okazaki 444-8585, Japan*
[3]*Department of Enviromental Science, Niigata University, Niigata 950-2181, Japan*

We compare here the Auger decay of a 3d hole in the same isoelectronic configuration $3d^{-1}4s^24p^6$ but in two different atoms. The aim is to test the influence of the nucleus charge Z. Namely we compare the decay of the $Kr^+$ $3d^{-1}4s^24p^6$ state (Z=36), created by photoionization of the Kr atom, with that of the Br $3d^{-1}4s^24p^6$ state (Z=35), created by ultra-fast dissociation of the HBr molecule upon 3d→σ* excitation [1].

The experiments were carried out on the soft X-ray beamline BL6U at UVSOR. The monochro- matized radiation was introduced into a gas cell filled with sample gas. Kinetic energies of the emitted electrons were measured by a hemispherical electron energy analyzer (MBS-A1) placed at a right angle relative to the photon beam direction. The axis of the electrostatic lens of the analyzer was set to be at the magic angle compared to the polarization direction of the incident light. The energy resolution of the analyzer was set to ~12 meV. The monochromator exit slit opening was set to 300 μm, which corresponds to a resolving power of ~1000.

Figure 1 displays a $Kr^+$ 3d Auger spectrum. It was obtained at 99 eV photon energy in order to avoid contamination by the decay of 3d satellite states. The main Auger lines are grouped in 3 zones, associated with the formation of the $Kr^{2+}$ final states of $4s^14p^5$, $4s^24p^34d$ and $4s^04p^6$ configurations [2]. The Double Auger decay produces electrons of 0 to ~22 eV [3].

The ultra-fast dissociation of the HBr 3d→ σ* resonance is known to produce an excited atomic Br* $3d^{-1}4s^24p^6$ fragment [1] after the dissociation. In 2012 we showed that the equipment at UVSOR allows one to measure the Auger electron spectrum of the Br* fragment with an unprecedented resolution. Here, we extend this work to the complete Auger spectrum. Figure 2 (top red) displays the result directly comparable to the $Kr^+$ case of Fig. 1, which was obtained by combining the measurements on the $3d_{3/2}$ and $3d_{5/2}$ → σ* resonances. One observes a similar distribution for the $Kr^{2+}$ and $Br^+$ final states of $4s^14p^5$ and $4s^04p^6$ configurations, but the structures of the 'satellite' states of a $4s^24p^34d$ configuration are richer in $Br^+$ than $Kr^{++}$, suggesting the sensitivity of the 4d orbital to the Z value of the core. Another marked difference is the energy region where double Auger decay contributes. From energetics reasons [4], it is expected to be wider in the Br case, producing electrons up to ~32 eV. The $4s^04p^6$ $Br^+$ states are thus predicted to decay further. Finally a measurement on the $3d_{5/2}$ → σ* resonance (Fig. 2, bottom) isolates the lines associated with the decays of the $3d_{5/2}$ hole, without the need of coincidence experiments used in the $Kr^+$ case [3].

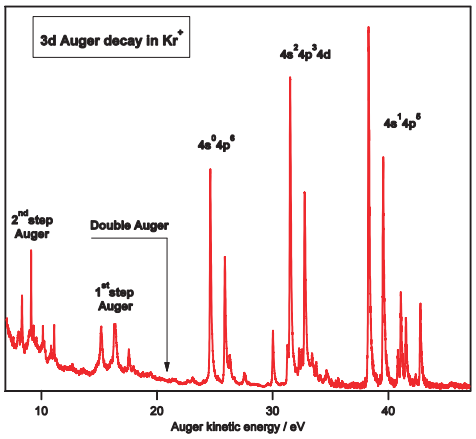


Fig. 1. Auger spectrum following the decays of a 3d hole in $Kr^+$ $3d^{-1}4s^24p^6$.

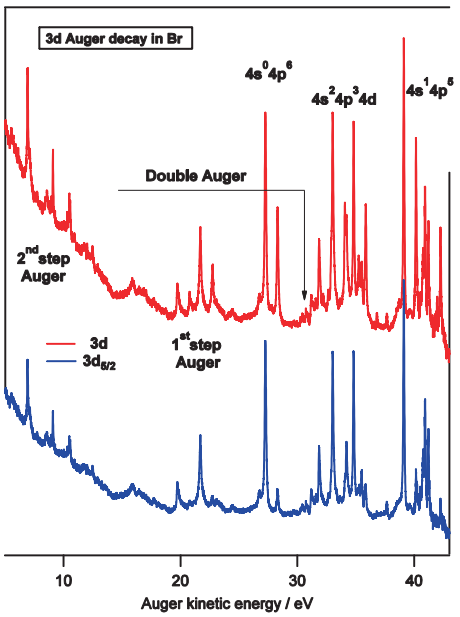


Fig. 2. Auger spectrum following the decays of a 3d hole in Br $3d^{-1}4s^24p^6$. Top (red) is directly comparable to the Kr case. Bottom (blue) was measured on the HBr $3d_{5/2}$ → σ* resonance and selects essentially the $3d_{5/2}$ hole decays.

[1] P. Morin and I. Nenner, PRL **56** (1986)1913.
[2] J. Jauhiainen *et al.*, J. Phys. B **28** (1995) 3831.
[3] J. Palaudoux *et al.*, PRA **82** (2010) 043419.
[4] http://physics.nist.gov/asd

BL8B

# Ultraviolet Photoelectron Spectra of $Tm_2@C_{82}$ (III) and $Tm_2C_2@C_{82}$ (III)

T. Miyazaki[1], Y. Tokumoto[1], R. Sumii[2,3], H. Yagi[1], N. Izumi[4], H. Shinohara[4] and S. Hino[1]
[1]*Graduate School of Science and Engineering, Ehime University, Matsuyama 790-8577, Japan*
[2]*Institutes for Molecular Science, Okazaki, 444-858, Japan*
[3]*Research Center for Materials Science, Nagoya University, Nagoya 464-8602, Japan*
[4]*Graduate School of Science, Nagoya University, Nagoya 464-8602, Japan*

Fullerenes cages often encapsulated metal atom(s) and metal-carbide clusters, and entrapped metal atom(s) donate electrons to the cage, which induce the change in their electronic structure. As for mono-metal atom and multiple atoms encapsulated $C_{82}$, the oxidation state of encapsulated metal atom is either +2 or +3. We have been measuring the ultraviolet photoelectron spectra (UPS) of endohedral metallofullerenes and revealed their valence band electronic structure [1-3]. In the course of the investigation a following empirical rule has been established: the UPS in the upper binding energy region ($E_b$ < 5 eV) were significantly different when either the cage structure or the amounts of transferred electrons is different. Recently, Tm atoms and $Tm_2C_2$ encapsulated $C_{82}$ fullerenes, $Tm_2@C_{82}$ (III) and $Tm_2C_2@C_{82}$ (III), have been isolated. In this report, the UPS of $Tm_2@C_{82}$ (III) and $Tm_2C_2@C_{82}$ (III) are presented and are compared with those of other endohedral fullerenes.

The UPS were measured at BL8B of UVSOR facility of Institute for Molecular Science. The base pressure of the UPS measurement chamber was $4\times10^{-8}$ Pa and the pressure during the measurement was about $6\times10^{-8}$ Pa. The measured UPS were referenced against the Fermi level ($E_F$) of gold and were plotted as a function of binding energy relative to $E_F$. All UPS were normalized by the peak height of a structure appeared at around 5.5 eV.

The UPS of $Tm_2@C_{82}$ (III) and $Tm_2C_2@C_{82}$ (III) obtained with $h\nu$ = 20 ~ 60 eV incident photon energy. The UPS of two metal atoms encapsulated endohedral fullerenes $Y_2@C_{82}$-$C_{3v}$, $Er_2@C_{82}$-$C_{3v}$ and $Tm_2@C_{82}$ (III) ($M_2$ group), and those of metal-carbide ($M_2C_2$) encapsulated metallofullerenes $Y_2C_2@C_{82}$-$C_{3v}$, $Er_2C_2@C_{82}$-$C_{3v}$ and $Tm_2C_2@C_{82}$ (III) ($M_2C_2$ group) obtained by 40eV photon energy are shown in Fig. 1 for comparison. The UPS of the $M_2$ group are almost identical; the peaks of structures A – C appear at the same binding energy region with almost the same intensity. Resemblance of these UPS suggests that the electronic structure of the $M_2$ group is almost identical. Since the electronic configuration of $Er_2@C_{82}$ and $Y_2@C_{82}$ was determined to be $M_2^{6+}@C_{82}^{6-}$, the oxidation state of Tm atom in $Tm_2@C_{82}$ can be deduced to be +3. This finding is rather surprising since the oxidation state of Tm atom in $Tm@C_{82}$ is +2. The UPS of the $M_2C_2$ group are also identical, which suggests their analogous electronic structure. The UPS of groups $M_2$ and $M_2C_2$ show good correspondence among them; three structures A – C appear at more or less the same energy region. The comparison of the UPS of $Y_2@C_{82}$ (II) and $Y_2C_2@C_{82}$ (II) suggested that the electronic configuration of $Y_2C_2@C_{82}$ is $(YC)_2^{4+}@C_{82}^{4+}$.

Present findings of the oxidation state of entrapped Tm atom(s) are rather surprising. The oxidation state of Tm atom is easily changed when the number of entrapped atoms is changed. When Y atom(s) are entrapped in the $C_{82}$ cage, the oxidation state of Y atom is +3, and it is independent on the number of entrapped atoms. The most stable oxidized form of a compromise to have the stable electronic states of the $C_{82}$ cage and Tm atoms.

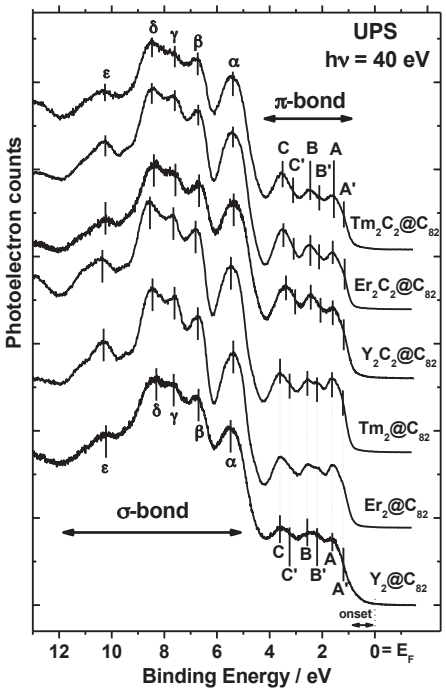


Fig. 1. UPS of $M_2@C_{82}$-$C_{3v}$ and $M_2C_2@C_{82}$-$C_{3v}$ (M=Y, Er, Tm) with $h\nu$ = 40 eV.

[1] S. Hino *et al.,* Bull. Chem. Soc. Jpn. **82**(2009) 963.
[2] T. Miyazaki *et al.,* Chem. Phys. **378** (2010) 11.
[3] T. Miyazaki *et al.,* Chem. Phys. **397** (2012) 87.

# One year of at UVSOR